

# WSI-SAM: Multi-resolution Segment Anything Model (SAM) for histopathology whole-slide images

Hong Liu<sup>\*,1</sup>, Haosen Yang<sup>\*,2</sup>, Paul J. van Diest<sup>3</sup>, Josien P.W. Pluim<sup>1</sup>, and Mitko Veta<sup>1</sup>

<sup>1</sup> Eindhoven University of Technology, Eindhoven, The Netherlands

<sup>2</sup> University of Surrey, London, UK

<sup>3</sup> University Medical Center Utrecht, University Utrecht, Utrecht, The Netherlands

\*Joint main authors-hong.liu.00408@gmail.com, haosen.yang.6@gmail.com

**Abstract.** The Segment Anything Model (SAM) marks a significant advancement in segmentation models, offering powerful zero-shot capabilities and dynamic prompting. However, existing medical SAMs are not suitable for the multi-scale nature of whole-slide images (WSIs), restricting their effectiveness. To resolve this drawback, we present WSI-SAM, enhancing SAM with precise object segmentation capabilities for histopathology images using multi-resolution patches, while preserving its original prompt-driven design, efficiency, and zero-shot adaptability. To fully exploit pretrained knowledge while minimizing training overhead, we keep SAM frozen, only introducing minimal additional parameters and computation. In particular, we introduce High-Resolution (HR) token, Low-Resolution (LR) token and dual mask decoder. This decoder integrates the original SAM mask decoder with a lightweight fusion module that integrates features at multiple scales. Instead of predicting a mask independently, we integrate HR and LR token at intermediate layer to jointly learn features of the same object across multiple resolutions. Experiments show that our WSI-SAM outperforms state-of-the-art SAM and its variants. In particular, our model outperforms SAM by 4.1 and 2.5 percent points on a ductal carcinoma in situ (DCIS) segmentation tasks and breast cancer metastasis segmentation task (CAMELYON16 dataset). The code will be available at <https://github.com/HongLiuuuuu/WSI-SAM>.

**Keywords:** Foundation Models · Computational pathology · Whole-slide images.

## 1 Introduction

Segmentation is crucial in histopathology images, enabling pathologists to analyze tissue regions such as tumor and stroma and in turn use those results for a number of tasks such as disease diagnosis, treatment planning, and monitoring progression. Current deep learning-based models [4,18,22,5,14,15,7] have

shown great promise in histopathology image segmentation, which can significantly reduce time, labor, and expertise required, and enable large-scale dataset analysis. However, these models are typically designed and trained for a specific segmentation task, which greatly limits the generalization to wider applications in clinical practice. Therefore, it is essential to develop universal models with zero-shot ability that can be trained once and then applied to a wide range of histopathology segmentation tasks.

Recently, the segment anything model (SAM) [10] was released as a segmentation foundation model for natural images, showcasing remarkable zero-shot abilities across various scenarios. Enabling its application across a wide range of tasks [13,2,17,23,11,3,1,25] through simple prompting, this breakthrough has catalyzed a significant paradigm shift. Some attempts have been made to apply SAM to histopathology images to boost the performance on various segmentation tasks. Med-SAM [12] fine-tunes the mask decoder of SAM on various medical datasets, while MedSAM Adapter [21] incorporates an adapter trained on diverse medical datasets. Although these methods show strong performance on particular tasks, we hypothesize that they are suboptimal in processing histopathology WSIs that possess a pyramid structure of multiple resolutions. For instance, to capture detailed information of ductal carcinoma in situ (DCIS) lesions, patches must be extracted from images as large as  $10,000 \times 10,000$  pixels at  $10\times$  magnification to manage costs [16,6] and ensure compatibility with SAM, which has an input resolution of  $1024 \times 1024$ . A single resolution SAM model might fail because more contextual information is needed in order to "understand" the object of interest is a lesion that should also include the lesion interior, as shown in Figure 1. More visualization results can be found in the supplementary materials.

To overcome the aforementioned limitation, in this work, we propose WSI-SAM, a model that leverages multi-resolution patches (i.e., subregions from a WSI) to perform segmentation in a zero-shot manner. Similar to HookNet [16], we extract a patch from a position within the WSI and couple it with a concentric lower-resolution patch to capture essential contextual information, as illustrated in Figure 1 (right). Instead of fusing the contextual information directly at the pixel level, we execute aggregation at the token level due to token represent the segmented object information in the SAM mask generation mechanism. We opt to aggregate contextual information at the token level instead of directly at the pixel level. This decision is based on the fact that tokens represent the information of segmented objects within the SAM mask generation framework. Considering that re-training the SAM model can severely degrade the general zero-shot performance [9], we propose the WSI-SAM architecture, which tightly integrates with and re-uses the existing learned SAM structure, in order to fully preserve the zero-shot performance. Specifically, we firstly introduce High-Resolution (HR) Token and Low-Resolution (LR) Token. Unlike the original output tokens, our HR and LR Token and their associated MLP layers are trained to predict masks of high-resolution and low-resolution patches. Secondly, we propose a dual mask decoder that integrates the original SAM mask decoder with a fusion module. The fusion module facilitates the fusion of global

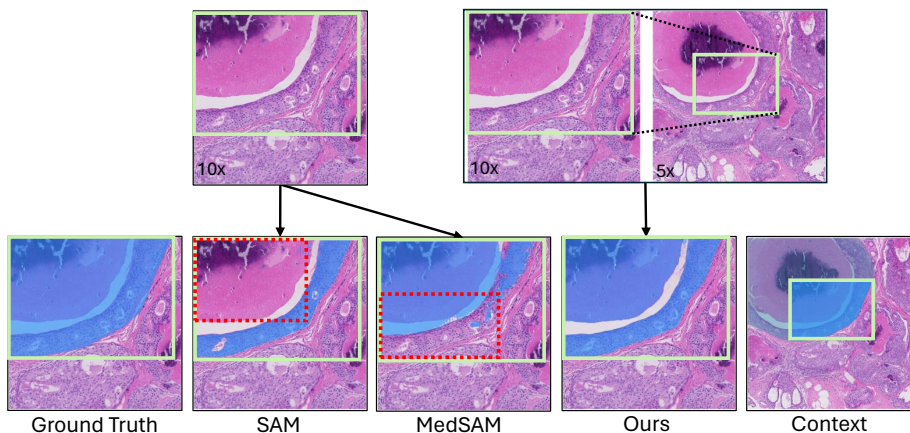


Fig. 1: Comparison of DCIS segmentation in H&E-stained breast tissue by SAM, MedSAM, and our WSI-SAM. Using the same green box as input prompt on a 10 $\times$  magnification patch, SAM erroneously does not segment the interior wall of DCIS lesion. This error is compounded by the presence of calcifications and necrosis in the interior of the duct. MedSAM overlooks the ductal region beneath the lumen. Leveraging additional context (right), our WSI-SAM predict more accurate entire DCIS area, despite the intervening background and dark region.

semantic context and local fine-grained features by fusing SAM’s mask decoder features with early and late feature maps from its ViT encoder. Finally, instead of predicting masks independently, we integrate the HR and LR tokens at the intermediate decoder layer for contextual information aggregation across both resolutions to generate accurate mask details.

Our contributions are summarized as follows: (1) This paper introduces WSI-SAM, a segmentation framework building upon SAM, designed to seamlessly integrate contextual cues with high-resolution details, enabling the prediction of the detailed segmentation mask for histopathology images in a zero-shot manner. (2) To achieve this objective, we introduce the High-Low Resolution Token, Dual Mask Decoder, and Token Aggregation, which together facilitate enhanced segmentation without the need for training from scratch. (3) The effectiveness of our method has been validated by two benchmarks, DCIS and CAMELYON16.

## 2 Method

### 2.1 Preliminary: SAM architecture

SAM comprises three core modules: (a) Image encoder: Utilizing a ViT-based backbone, this module extracts image features, yielding image embeddings. (b) Prompt encoder: It encodes positional information from input points, boxes, or masks to facilitate the mask decoder. (c) Mask decoder: This transformer-based decoder leverages both the extracted image embeddings and prompt tokens to make final mask predictions. One of SAM’s remarkable features is its robust

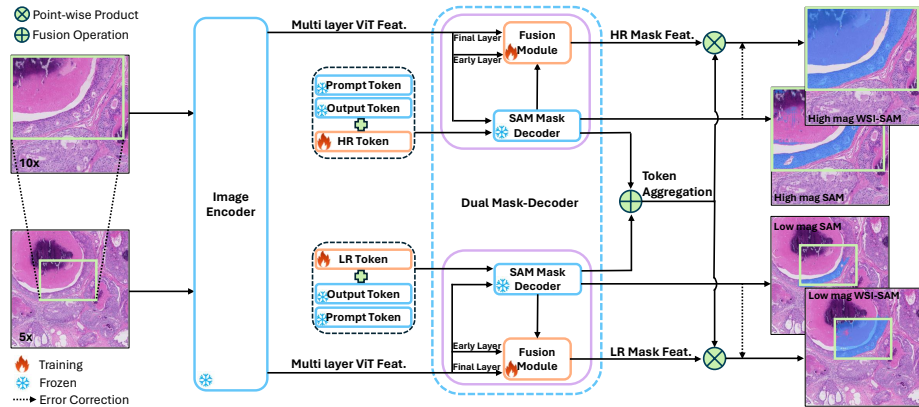


Fig. 2: WSI-SAM model architecture, which introduces HR and LR Tokens, Dual Mask Decoder and Token Aggregation to SAM for improving the mask quality in histopathology WSIs.

zero-shot generalization to novel scenarios, thanks to extensive training on a vast repository of prompt-mask pairs.

## 2.2 Ours: WSI-SAM

To preserve the zero-shot transfer capability of SAM, while preventing model overfitting or catastrophic forgetting, instead of directly finetuning SAM or adding a new heavy decoder network, we take a minimal adaptation approach as much as possible. To this end, we introduce three novel components in our WSI-SAM, as illustrated in Figure 2.

*High and Low Resolution Tokens* We propose efficient adaptation for improving the mask quality in histopathology WSIs. As shown in Figure 2, the output token is adopted for mask prediction [10], which predicts dynamic MLP weights and then performs point-wise product with the mask features. To promote SAM’s mask quality in WSIs, instead of directly taking SAM’s coarse masks as input, we introduce High Resolution (HR) and Low Resolution (LR) Tokens, accompanied by a corresponding new mask prediction layer, to facilitate mask prediction across multiple resolutions. In Figure 2, by reusing and fixing SAM’s mask decoder, two new learnable HR and LR Tokens (size of  $1 \times 256$  for each) are concatenated with SAM’s output tokens (size of  $4 \times 256$ ) and prompt tokens (size of  $N_{prompt} \times 256$ ) as the input to the SAM’s mask decoder. Similar to the original output token, the HR and LR Tokens interact with their corresponding resolution image features for its feature updating.

*Dual Mask Decoder* To achieve the best interaction between Token and ViT features, we propose dual mask decoder, which include the SAM mask decoder

and a lightweight fusion module. HR and LR Tokens use the point-wise MLP shared by the other tokens in each mask decoder layer. Once processed through the mask decoder layers, the updated HR and LR Tokens acquire comprehensive insights into the global image context, crucial geometric/type information conveyed by prompt tokens, and hidden mask details inherent in the output token. To further promote mask quality, we enrich both the high-level object context and low-level boundary/edge information in the mask decoder features of SAM at Fusion modules. Specifically, we compose the new features by extracting and fusing features from different stages of the SAM model, which includes features from both early and late layers of the ViT, as well as mask features derived from the mask decoder.

*Token Aggregation* Rather than predicting the mask independently, we introduce Token Aggregation to capture contextual information across multiple resolutions, thereby enhancing mask detail accuracy. Specifically, we merge detailed features from the updated HR Token with broader contextual features from the LR Token, as these tokens encapsulate features of the same object at different resolutions. As illustrated in Figure 2, the merge operation is formed by averaging the updated HR and LR Tokens. This Aggregation method is both simple and effective, yielding segmentation results that preserve detail while requiring minimal memory and computational resources. Subsequently, a spatial point-wise product is applied to the HR and LR mask features to facilitate mask generation.

### 2.3 Training Objective

While training WSI-SAM, a separate loss is computed for each resolution. We propose a loss function

$$L = \lambda L_{high} + (1 - \lambda)L_{low},$$

where  $L_{high}$  and  $L_{low}$  are the combination of dice loss and cross-entropy loss for different resolutions, respectively, and  $\lambda$  controls the importance of each resolution.

## 3 Experiments and Results

*Training data* To train WSI-SAM in a data-efficient manner, we train on the **CATCH** [20] dataset. This dataset contain 350 WSIs of seven distinct subtypes of canine cutaneous tumors, augmented with 12,424 polygon annotations across 13 histological classes. Following the official division, the dataset is split into a training set with 245 WSIs and a validation set encompassing 35 WSIs.

*Benchmark settings* We assess our model’s performance on two Whole Slide Image (WSI) datasets in a zero-shot manner. The first is a dataset of Ductal Carcinoma in Situ (**DCIS** [19]), a non-invasive breast cancer collection comprising 116 WSIs. From this, 50 WSIs were randomly selected for our test set. The

second is the **CAMELYON16**<sup>1</sup> dataset, where we incorporated its official test set into our own. This set includes a total of 47 WSIs.

### 3.1 Implementation Details

During training, we fix the model parameters of the pre-trained SAM model while only making the proposed WSI-SAM learnable. Since SAM is designed for flexible segmentation prompts, we train WSI-SAM by sampling mixed types of prompts including bounding boxes, randomly sampled points, and coarse masks. We generate these degraded masks by adding random Gaussian noise in the boundary regions of the GT masks. Given hardware constraints, we randomly select a limited number of  $1024 \times 1024$  patches at  $10\times$  magnification and their corresponding concentric patches at  $5\times$  magnification from each WSI for training. We adopt TinyViT [24] as its backbone. Our training employs a mini-batch size of 1 and a learning rate 0.001. We conducted all experiments using PyTorch on a setup equipped with an NVIDIA TITAN Xp GPU.

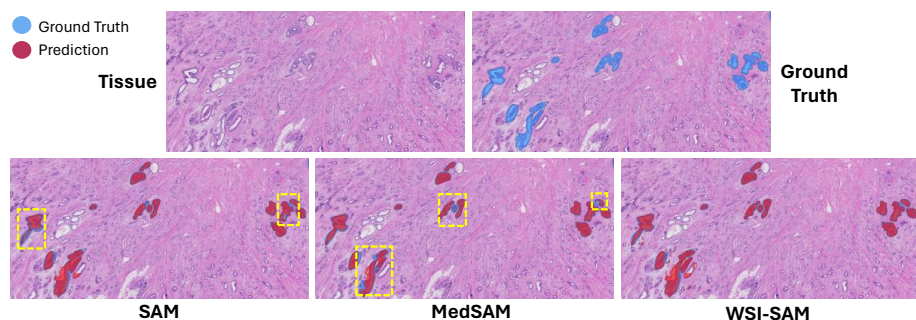


Fig. 3: Example of predicted tissue segmentation on DCIS. Yellow boxes indicate the incorrect predictions.

### 3.2 Zero-shot Comparison with SAMs

*Setup* In our evaluation process, we conduct zero-shot mask prediction using prompts. Our investigation includes two distinct types of prompts: box and point. To precisely measure enhancements in mask quality, we utilize the dice score as our reporting metric.

*Zero shot segmentation with box prompt* We compare with SAM, finetuned SAM and MedSAM on both DCIS and CAMELYON16 datasets. We simulate realistic human-annotated bounding boxes by introducing noise to the GT object boxes. As shown in Table 1, we observe a marked decrease in performance when fine-tuning SAM on histopathology WSIs, attributed to the disruption of pre-trained knowledge through fine-tuning. In contrast, WSI-SAM outperforms SAM

<sup>1</sup> <https://camelyon17.grand-challenge.org/Data/>

Table 1: Comparison of zero-shot segmentation results on the DCIS and CAMELYON16 test sets using bounding boxes as input prompts. \* indicate finetune SAM’s mask decoder on CATCH

Method	DCIS	CAMELYON16			
	DCIS	IDC	ILC	DUC	avg
SAM [10]	73.35	86.06	81.36	72.86	80.09
SAM*	61.22	74.17	72.88	40.00	62.35
MedSAM [12]	64.71	77.91	75.24	71.64	74.93
WSI-SAM (Ours)	<b>77.50</b>	<b>89.76</b>	<b>84.30</b>	<b>73.55</b>	<b>82.54</b>

by 4.1 and 2.5 percent points on the DCIS and CAMELYON16 datasets, respectively. Furthermore, when compared to MedSAM, which was trained on a variety of medical datasets, WSI-SAM demonstrates a significant performance enhancement, as evidenced by the substantial increase from **64.71%** to **77.50%**. Moreover, to simulate real-world scenarios, we further evaluated our method using prompts generated from nnU-Net [8]. WSI-SAM surpasses both SAM and MedSAM (e.g., **56.0**, **56.73** vs **59.9**), showcasing the resilience and robustness of our approach. To provide additional validation, we conduct a segmentation qualitative analysis on DICS, as illustrated in Figure 3.

Table 2: Zero-shot segmentation result comparison on the test set of DCIS. We use nnU-Net [8] trained on DCIS as box prompt generator.

Method	SAM	MedSAM	WSI-SAM
Dice	56.00	56.43	<b>57.37</b>

*Zero shot segmentation with point prompt* To investigate the segmentation capabilities of WSI-SAM using interactive point prompts, we conducted a comparison with SAM, evaluating their performances across a range of input point quantities on both the DCIS and CAMELYON16 datasets. Noting that MedSAM is limited to box prompts. For the CAMELYON16 dataset, we present an average performance across the three tumor classes, with comprehensive metrics for each class detailed in the supplementary materials. WSI-SAM consistently outperforms SAM on both datasets, regardless of the number of point prompts utilized, as shown in the Figure 4.

### 3.3 Ablation Study

We conducted an ablation study for WSI-SAM on DCIS dataset with bounding boxes as input prompts.

*Effect of the HR and LR Tokens.* WSI-SAM leverages HR and LR Tokens to fuse more contextual information, enhancing mask prediction accuracy. We examined various aggregation target, specifically (1) fuse the high and low feature by average-pooling, fuse with expand feature region on the high-resolution features and high and low token aggregation. Results presented in Table 3b indicate

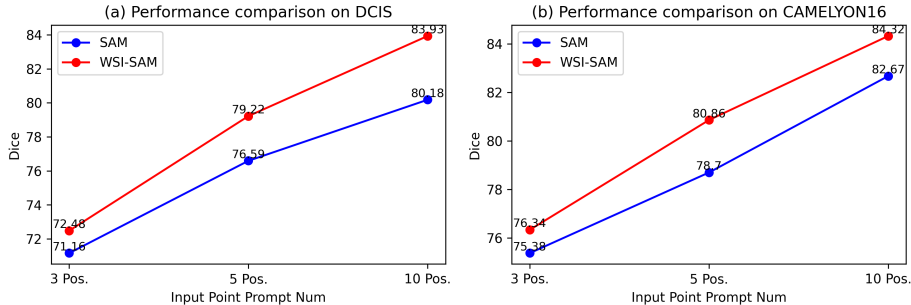


Fig. 4: Zero-shot interactive segmentation results comparison using a varying number of input points on the DCIS and CAMELYON16 dataset.

that utilizing HR and LR Tokens, consistently outperforms these alternatives, achieving performance improvements of 5.3 percent points on DCIS dataset.

*Ablation on Tokens Aggregation* We evaluate three ways of fusing HR and LR Tokens: (1) Concatenating followed by one learnable FC layer (Concat-FC); (2) Max pooling (Max); (3) Average pooling (Avg). Table 3a shows that the average pooling turns out to be the best way for aggregation.

Table 3: **Ablation experiments on DCIS dataset.** (a) Ablation study on aggregation ways for HR and LR Tokens using box prompts; (b) Ablation study on aggregation target for integrating contextual information using box prompts; (c) Ablation study on different values of  $\lambda$  in loss function.

(a)		(b)		(c)	
Aggregation	Dice	Aggregation Target	Dice	$\lambda$	Dice
Concat.-FC	77.24	HR feat. and LR feat.	72.20	0.25	76.65
Max.	75.91	HR feat. and expand HR feat.	59.04	0.5	<b>77.50</b>
Avg.	<b>77.50</b>	HR Token and LR Token	<b>77.50</b>	0.75	76.52

*Ablation on  $\lambda$  in loss function.* The influence of losses from HR and LR Tokens is modulated by  $\lambda$ . Experiments were conducted with  $\lambda = 0.25$  to favor the LR Token,  $\lambda = 0.5$  to balance both tokens equally, and  $\lambda = 0.75$  to prioritize the HR Token. According to Table 3c, setting  $\lambda = 0.5$  yields the best performance enhancement.

## 4 Conclusion

We introduce WSI-SAM, the zero-shot segmentation model tailored for WSIs, incorporating innovative HR and LR Tokens to refine the mask prediction of SAM’s output token and enhancing the original SAM with minimal additional computational cost. Our zero-shot transfer evaluations on the DCIS and CAMELYON16 datasets showcase WSI-SAM’s superior performance, marking a substantial advancement in zero-shot segmentation for WSIs.

## References

1. Chen, C., Miao, J., Wu, D., Yan, Z., Kim, S., Hu, J., Zhong, A., Liu, Z., Sun, L., Li, X., Liu, T., Heng, P.A., Li, Q.: Ma-sam: Modality-agnostic sam adaptation for 3d medical image segmentation. arXiv:2309.08842 (2023), arXiv preprint.
2. Cheng, J., Ye, J., Deng, Z., Chen, J., Li, T., Wang, H., Su, Y., Huang, Z., Chen, J., Jiang, L., Sun, H., He, J., Zhang, S., Zhu, M., Qiao, Y.: Sam-med2d. arXiv:2308.16184 (2023), arXiv preprint.
3. Fazekas, B., Morano, J., Lachinov, D., Aresta, G., Bogunović, H.: Samedoct: Adapting segment anything model (sam) for retinal oct. arXiv:2308.09331 (2023), arXiv preprint.
4. Feng, R., Liu, X., Chen, J., Chen, D.Z., Gao, H., Wu, J.: A deep learning approach for colonoscopy pathology wsi analysis: Accurate segmentation and classification. *IEEE Journal of Biomedical and Health Informatics* **25**(10), 3700–3708 (2021). <https://doi.org/10.1109/JBHI.2020.3040269>
5. Feng, Y., Hafiane, A., Laurent, H.: A deep learning based multiscale approach to segment the areas of interest in whole slide images. *Computerized Medical Imaging and Graphics* **90**, 101923 (2021). <https://doi.org/https://doi.org/10.1016/j.compedimag.2021.101923>
6. Gu, F., Burlutskiy, N., Andersson, M., Wilén, L.K.: Multi-resolution networks for semantic segmentation in whole slide images. In: *Computational Pathology and Ophthalmic Medical Image Analysis*. pp. 11–18. Springer International Publishing (2018)
7. Han, C., Lin, J., Mai, J., Wang, Y., Zhang, Q., Zhao, B., Chen, X., Pan, X., Shi, Z., Xu, Z., Yao, S., Yan, L., Lin, H., Huang, X., Liang, C., Han, G., Liu, Z.: Multi-layer pseudo-supervision for histopathology tissue semantic segmentation using patch-level classification labels. *Medical Image Analysis* **80**, 102487 (2022). <https://doi.org/https://doi.org/10.1016/j.media.2022.102487>
8. Isensee, F., Jaeger, P.F., Kohl, S.A.A., Petersen, J., Maier-Hein, K.H.: nnU-Net: a self-configuring method for deep learning-based biomedical image segmentation. *Nature Methods* **18**(2), 203–211 (2021). <https://doi.org/10.1038/s41592-020-01008-z>
9. Ke, L., Ye, M., Danelljan, M., Liu, Y., Tai, Y.W., Tang, C.K., Yu, F.: Segment anything in high quality. In: *Advances in Neural Information Processing Systems*. vol. 36, pp. 29914–29934 (2023)
10. Kirillov, A., Mintun, E., Ravi, N., Mao, H., Rolland, C., Gustafson, L., Xiao, T., Whitehead, S., Berg, A.C., Lo, W.Y., Dollár, P., Girshick, R.: Segment anything. In: *2023 IEEE/CVF International Conference on Computer Vision (ICCV)*. pp. 3992–4003 (2023). <https://doi.org/10.1109/ICCV51070.2023.00371>
11. Lei, W., Wei, X., Zhang, X., Li, K., Zhang, S.: Medlsam: Localize and segment anything model for 3d ct images. arXiv:2306.14752 (2023), arXiv preprint.
12. Ma, J., He, Y., Li, F., Han, L., You, C., Wang, B.: Segment anything in medical images. *Nature Communications* **15**, 1–9 (2024)
13. Mazurowski, M.A., Dong, H., Gu, H., Yang, J., Konz, N., Zhang, Y.: Segment anything model for medical image analysis: An experimental study. *Medical Image Analysis* **89**, 102918 (2023). <https://doi.org/https://doi.org/10.1016/j.media.2023.102918>
14. Ni, H., Liu, H., Wang, K., Wang, X., Zhou, X., Qian, Y.: Wsi-net: Branch-based and hierarchy-aware network for segmentation and classification of breast histopathological whole-slide images. In: *Machine Learning in Medical Imaging*. pp. 36–44. Springer International Publishing (2019)

15. Qaiser, T., Tsang, Y.W., Taniyama, D., Sakamoto, N., Nakane, K., Epstein, D., Rajpoot, N.: Fast and accurate tumor segmentation of histology images using persistent homology and deep convolutional features. *Medical Image Analysis* **55**, 1–14 (2019). <https://doi.org/https://doi.org/10.1016/j.media.2019.03.014>
16. van Rijthoven, M., Balkenhol, M., Siliņa, K., van der Laak, J., Ciompi, F.: Hooknet: Multi-resolution convolutional neural networks for semantic segmentation in histopathology whole-slide images. *Medical Image Analysis* **68**, 101890 (2021). <https://doi.org/https://doi.org/10.1016/j.media.2020.101890>
17. Wang, H., Guo, S., Ye, J., Deng, Z., Cheng, J., Li, T., Chen, J., Su, Y., Huang, Z., Shen, Y., Fu, B., Zhang, S., He, J., Qiao, Y.: Sam-med3d. arXiv:2310.15161 (2023), arXiv preprint.
18. Wang, X., Fang, Y., Yang, S., Zhu, D., Wang, M., Zhang, J., Yu Tong, K., Han, X.: A hybrid network for automatic hepatocellular carcinoma segmentation in h&e-stained whole slide images. *Medical Image Analysis* **68**, 101914 (2021). <https://doi.org/https://doi.org/10.1016/j.media.2020.101914>
19. Wetstein, S.C., Stathonikos, N., Pluim, J.P., Heng, Y.J., ter Hoeve, N.D., Vreuls, C.P., van Diest, P.J., Veta, M.: Deep learning-based grading of ductal carcinoma in situ in breast histopathology images. *Laboratory Investigation* **101**(4), 525–533 (2021). <https://doi.org/https://doi.org/10.1038/s41374-021-00540-6>
20. Wilm, F., Fragoso, M., Marzahl, C., Qiu, J., Puget, C., Diehl, L., Bertram, C.A., Klopffleisch, R., Maier, A., Breining, K., Aubreville, M.: Pan-tumor canine cutaneous cancer histology (catch) dataset. *Scientific Data* **9**(1), 588 (2022). <https://doi.org/10.1038/s41597-022-01692-w>
21. Wu, J., Ji, W., Liu, Y., Fu, H., Xu, M., Xu, Y., Jin, Y.: Medical sam adapter: Adapting segment anything model for medical image segmentation. arXiv:2304.12620 (2023), arXiv preprint.
22. Xu, G., Song, Z., Sun, Z., Ku, C., Yang, Z., Liu, C., Wang, S., Ma, J., Xu, W.: Camel: A weakly supervised learning framework for histopathology image segmentation. In: 2019 IEEE/CVF International Conference on Computer Vision (ICCV). pp. 10681–10690 (2019). <https://doi.org/10.1109/ICCV.2019.01078>
23. Yue, W., Zhang, J., Hu, K., Xia, Y., Luo, J., Wang, Z.: Surgicalsam: Efficient class promptable surgical instrument segmentation. arXiv:2308.08746 (2023), arXiv preprint.
24. Zhang, C., Han, D., Zheng, S., Choi, J., Kim, T.H., Hong, C.S.: Mobilesamv2: Faster segment anything to everything. arXiv:2312.09579 (2023), arXiv preprint.
25. Zhang, Y., Cheng, Y., Qi, Y.: Semisam: Exploring sam for enhancing semi-supervised medical image segmentation with extremely limited annotations. arXiv:2312.06316 (2023), arXiv preprint.

## Appendix

Table 4: **Comparison of zero-shot segmentation results on CAMELYON16 test sets using different numbers of points as input prompts. (a) 3 positive points; (b) 5 positive points; (c) 10 positive points.**

(a)

Method	IDC	ILC	DUC
SAM	85.26	80.76	60.13
WSI-SAM	<b>85.63</b>	<b>81.66</b>	<b>61.73</b>

(b)

Method	IDC	ILC	DUC
SAM	87.53	82.09	66.48
WSI-SAM	<b>89.53</b>	<b>84.90</b>	<b>68.16</b>

(c)

Method	IDC	ILC	DUC
SAM	89.43	83.97	74.61
WSI-SAM	<b>91.53</b>	<b>86.23</b>	<b>75.22</b>

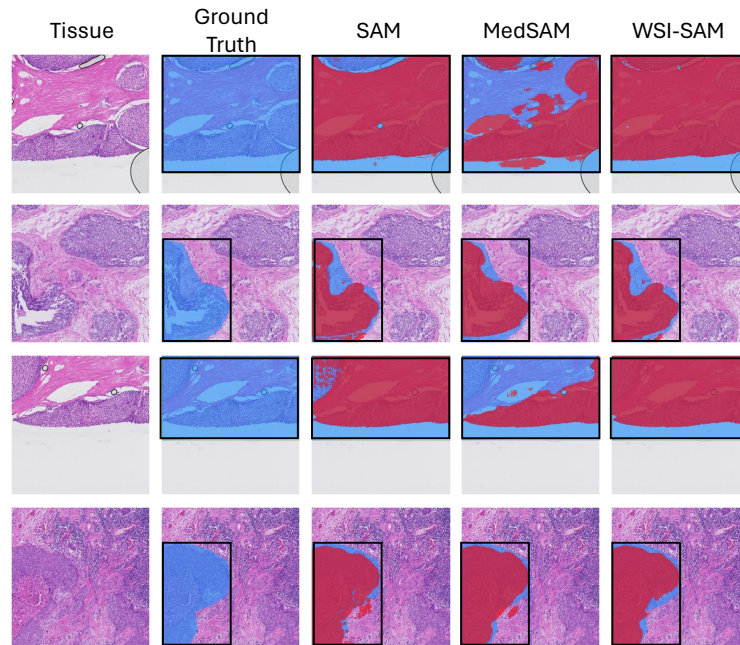


Fig. 5: Comparison of segmentation mask predictions in DCIS dataset.

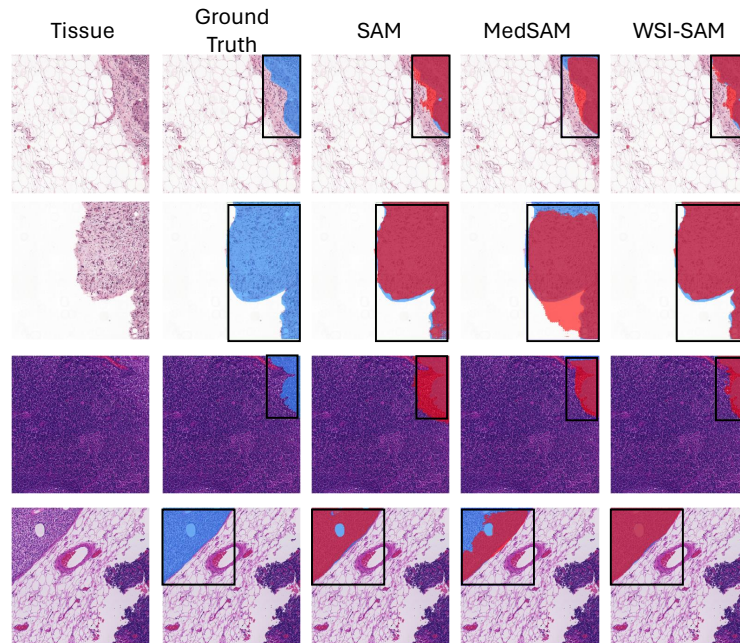


Fig. 6: Comparison of segmentation mask predictions in CAMELYON16 dataset.